Intense emission of Ba2MgSi2O7:Eu2+ under X-ray excitation for potential detecting applications

Yan, Jing; Liu, Chunmeng; Vlieland, John; Zhou, Jiabang; Dorenbos, Pieter; Huang, Yan; Tao, Ye; Liang, Hongbin

DOI
10.1016/j.jlumin.2016.11.009

Publication date
2017

Document Version
Final published version

Published in
Journal of Luminescence

Journal of Luminescence 183 (2017) 97–101

Contents lists available at ScienceDirect

Journal of Luminescence

journal homepage: www.elsevier.com/locate/jlumin

Intense emission of $Ba_2MgSi_2O_7:Eu^{2+}$ under X-ray excitation for potential detecting applications

Jing Yan [a], Chunmeng Liu [a], John Vlieland [b], Jianbang Zhou [a], Pieter Dorenbos [b], Yan Huang [c], Ye Tao [c], Hongbin Liang [a,*]

[a] MOE Key Laboratory of Bioinorganic and Synthetic Chemistry, KLGHEI of Environment and Energy Chemistry, School of Chemistry, Sun Yat-sen University, Guangzhou 510275, China
[b] Faculty of Applied Sciences, Delft University of Technology, Mekelweg 15, 2629 JB Delft, The Netherlands
[c] Beijing Synchrotron Radiation Facility, Institute of High Energy Physics, Chinese Academy of Sciences, Beijing 100039, China

ARTICLE INFO

Article history:
Received 5 May 2016
Received in revised form
5 November 2016
Accepted 7 November 2016
Available online 16 November 2016

Keywords:
$Ba_2MgSi_2O_7$
Photoluminescence
Radioluminescence
Thermoluminescence
Light yield
Scintillation material

ABSTRACT

A series of $Ba_{2-x}Eu_xMgSi_2O_7$ phosphors was prepared by a solid-state reaction method at high temperature. The theoretical density of the optimal $Ba_{1.93}Eu_{0.07}MgSi_2O_7$ material was calculated from the Rietveld refinement result. Eu L_3-edge X-ray absorption near edge structure (XANES) spectrum was measured to confirm the valence of Eu ions in $Ba_2MgSi_2O_7$. The X-ray excited radioluminescence and the thermoluminescence after β-ray irradiation were investigated based on the VUV-vis photoluminescence. The light yield of the optimal $Ba_{1.93}Eu_{0.07}MgSi_2O_7$ sample under X-ray excitation was estimated to be ~29,000 ± 6000 photons/M eV. So the temperature-dependent luminescence properties of this sample under X-ray and 344 nm excitation were further studied, and the charge traps in the scintillation process were discussed through thermoluminescence spectra. The high scintillation intensity together with an appropriate intrinsic decay time and its non-hygroscopicity endow the further optimized phosphor $Ba_{1.93}Eu_{0.07}MgSi_2O_7$ a promising scintillation material for X-ray detection.

1. Introduction

Nowadays, much attention is being addressed to f-d transitions of lanthanide ions in different hosts for applications in lighting and displays [1–3]. As important host compounds of luminescence of lanthanide or transition metal ions, silicates have attracted much attention due to their good chemical and thermal stabilities [4–8]. Eu^{2+} ions have $4f^7$ ground and $4f^65d$ excited states, the parity allowed $4f^65d \rightarrow 4f^7$ transitions exhibit broad emission bands with decay times typically about 500 ns to 1 μs [9]. Thus Eu^{2+} doped materials may also have potential applications as scintillators [9–11]. Although Ce^{3+} doped luminescent materials are applied as scintillators to detect X/γ rays or thermal neutrons due to the fast Ce^{3+} decay characteristic, Eu^{2+} doped luminescent materials are less frequently reported for scintillators application [9,10].

The synthesis and characterization of Eu^{2+} doped $Ba_2MgSi_2O_7$ phosphors have been reported, but most of the work just focused on the photoluminescence properties [4–7]. In this article, the luminescence properties of Eu^{2+} doped $Ba_2MgSi_2O_7$ under VUV – UV (vacuum ultraviolet – ultraviolet) and X-ray excitation were reported. We will address the high scintillation intensity of $Ba_{1.93}Eu_{0.07}MgSi_2O_7$ and the role of charge carrier traps in the scintillation process under X-ray excitation at different temperatures.

2. Experimental

The polycrystalline luminescent materials $Ba_{2-x}Eu_xMgSi_2O_7$ (x=0.01, 0.07, 0.10) were prepared by a high temperature solid state reaction method in a CO reducing ambient which was generated from the incomplete combustion of thermal carbon. The starting materials were $BaCO_3$ (analytical reagent, A.R.), MgO (A.R.), SiO_2 (A.R.) and Eu_2O_3 (99.99%). After these raw materials were weighed stoichiometrically and mixed thoroughly in an agate mortar, they were pre-fired at 1073 K for 2 h and then reground and sintered at 1543 K for 5 h to obtain final products.

The phase purity and structure of the final products were checked by X-ray powder diffraction (XRD) using a D8 ADVANCE diffractometer with CuKα radiation (λ=0.15418 nm) at room temperature (RT). The Eu L_3-edge XANES spectra were collected on Shanghai Synchrotron Radiation Facility (SSRF) in a transmission mode. All spectra were achieved on BL14W beam line of the storage ring operating at 3.5 G eV with an optimal current around

* Corresponding author.
E-mail address: cesbin@mail.sysu.edu.cn (H. Liang).

http://dx.doi.org/10.1016/j.jlumin.2016.11.009
0022-2313/

220 mA at RT. A liquid-He-cooled Si(111) double crystal monochromator was used in measurement. The ionization chamber with constant temperature at 298 K contained argon and nitrogen. The luminescent spectra in the UV–vis range and the decay curves were recorded with an Edinburgh Instruments FLS 920 combined fluorescence lifetime and steady-state spectrometer which was equipped with a time-correlated single-photon counting (TCSPC) card. The instrument was equipped with a CTI-Cryogenics temperature control system. A 450 W xenon lamp was used as the excitation source for the UV–vis spectra recording, the excitation photons for the luminescence decay curves collecting were provided by a 150 W F900 flash lamp with a pulse width of 1 ns and pulse rate of 40–100 Hz at RT. The VUV excitation and corresponding emission spectra were measured at the VUV spectroscopy experimental station on beam line 4B8 of the Beijing Synchrotron Radiation Facility. The emission spectra under X-ray excitation at RT and different temperatures, and thermoluminescence spectra were recorded by facilities at Delft University of Technology, The Netherlands [11]. The measurement and estimation of the light yield under X-ray excitation have been described in detail in our previous work [12].

3. Results and discussion

$M_2MgSi_2O_7$ (M=Ca, Sr, Ba) compounds have been identified to crystalize in tetragonal and monoclinic systems, respectively [4–6,13–18]. For our synthesized samples, XRD patterns of $Ba_2MgSi_2O_7$:Eu^{2+} are consistent with the monoclinic $Ba_2MgSi_2O_7$ [7,8]. To calculate the theoretical density, which is one of the main parameters of scintillation materials, the Rietveld refinement was performed for $Ba_{1.93}Eu_{0.07}MgSi_2O_7$ sample using the C2/c structure model as shown in Fig. 1[19]. The as-obtained goodness of fit parameters R_{wp}=2.06% R_p=1.31%, and R_B=0.98% can confirm the structure of our synthesized samples belong to the monoclinic system. The final refined structural parameters for $Ba_{1.93}Eu_{0.07}MgSi_2O_7$ are summarized in Table 1 and the theoretical density is calculated to be about 4.36 g/cm^3 according to the refinement result. Furthermore, another important parameter of scintillation materials, the effective atomic number (Z_{eff}) of $Ba_2MgSi_2O_7$ is estimated to be ~45.5 [20].

To confirm the valence of Eu ions in $Ba_2MgSi_2O_7$, the Eu L_3 edge

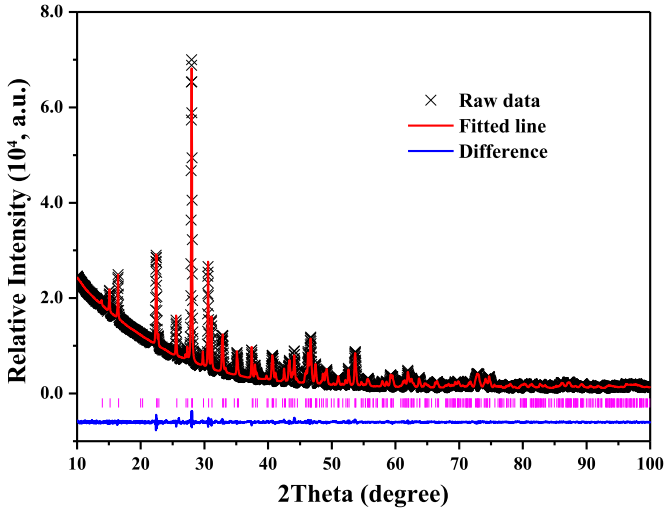

Fig. 1. The experimental (crosses) and calculated (red solid line) XRD patterns and their difference (blue solid line) of $Ba_{1.93}Eu_{0.07}MgSi_2O_7$. The pink ticks mark the Bragg reflection positions. (For interpretation of the references to color in this figure legend, the reader is referred to the web version of this article.)

Table 1
Final refined structural parameters for $Ba_{1.93}Eu_{0.07}MgSi_2O_7$[a].

Atoms	Site	x	y	z	Occ.	B_{iso} (Å^2)
Ba1	8f	0.2727(1)	0.45580(9)	0.0250(1)	0.965	1.020(9)
Eu1	8f	0.2727(1)	0.45580(9)	0.0250(1)	0.035	1.020(9)
Mg1	4e	0	0.2576(7)	0.25	1	1.00(7)
Si1	8f	0.8867(7)	0.2816(3)	−0.1375(6)	1	1.19(6)
O1	4e	0	0.3343(9)	−0.25	1	1.16(7)
O2	8f	0.704(1)	0.3459(8)	−0.232(1)	1	1.16(7)
O3	8f	0.974(1)	0.3488(9)	0.041(1)	1	1.16(7)
O4	8f	0.900(1)	0.1354(6)	−0.133(1)	1	1.16(7)

[a] Symmetry, monoclinic; space group, C2/c; Z=4; a=8.4174(1) Å, b=10.7184(1) Å, c=8.4525(1) Å, β=110.7604(8) and V=713.08(2) Å^3; ρ=4.36 g/cm^{-3}. The occupancy factors for Ba/Eu were fixed as 0.965/0.035 according to the nominal composition in the refinement.

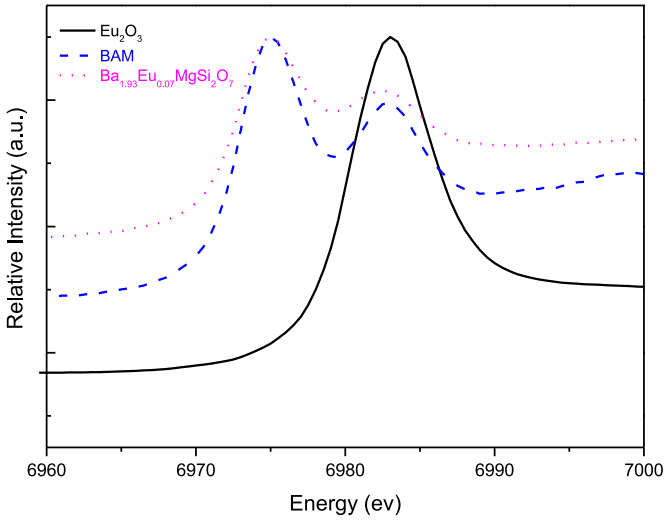

Fig. 2. The XANES spectra at Eu-L_3 edge of $Ba_{1.93}Eu_{0.07}MgSi_2O_7$, commercial $BaMgAl_{10}O_{17}$:Eu^{2+} (BAM) and Eu_2O_3 at RT.

X-ray absorption near edge structure (XANES) spectrum of $Ba_{1.93}Eu_{0.07}MgSi_2O_7$ was measured and compared with that of commercial $BaMgAl_{10}O_{17}$:Eu^{2+} (BAM) and Eu_2O_3 at RT as shown in Fig. 2. The absorption peak at ~6983 eV in XANES spectrum of Eu_2O_3 (black solid curve) is due to so-called "white line" coupled to the absorption of L_3 edge of Eu^{3+}, and that at ~6975 eV in other two curves is due to the absorption of L_3 edge of Eu^{2+}[21]. The results indicate that Eu^{2+} occurs together with Eu^{3+} in $Ba_{1.93}Eu_{0.07}MgSi_2O_7$.

The photoluminescence, cathodoluminescence and electronic properties of $Ba_{2-x}Eu_xMgSi_2O_7$ have been reported in our previous work [7]. Fig. 3(a) shows the synchrotron radiation VUV-UV (black solid line) and lab UV–vis (red dash line) excitation spectra of $Ba_{1.9}Eu_{0.1}MgSi_2O_7$ by monitoring Eu^{2+} 501 nm emission at RT. The host excitonic absorption band can be observed below 200 nm with a maximum at about 180 nm. The broad band from 200 to 450 nm corresponds to the $4f^7 \rightarrow 4f^6 5d$ transitions of Eu^{2+} in $Ba_2MgSi_2O_7$. Two factors, the crystal field splitting of Eu^{2+} 5d state and the ^7F_J (J=0, …, 6) multiplets arising from the spin-orbit coupling of remaining $4f^6$ core in the excited state of Eu^{2+}, play a significant role in the shape of the f-d bands in excitation spectra. Since Eu^{2+} ions occupy Ba^{2+} sites with C_1 symmetry in the host compound, five f-d excitation bands would appear when we do not consider the coulomb interaction between $4f^6$ and 5d electrons to a first approximation, due to crystal field splitting of Eu^{2+} 5d state in this low symmetry site [22]. The unresolved bands in this range may first result from the overlapping of five f-d excitation bands. Furthermore, the fine ^7F_J (J=0, …, 6) structure may

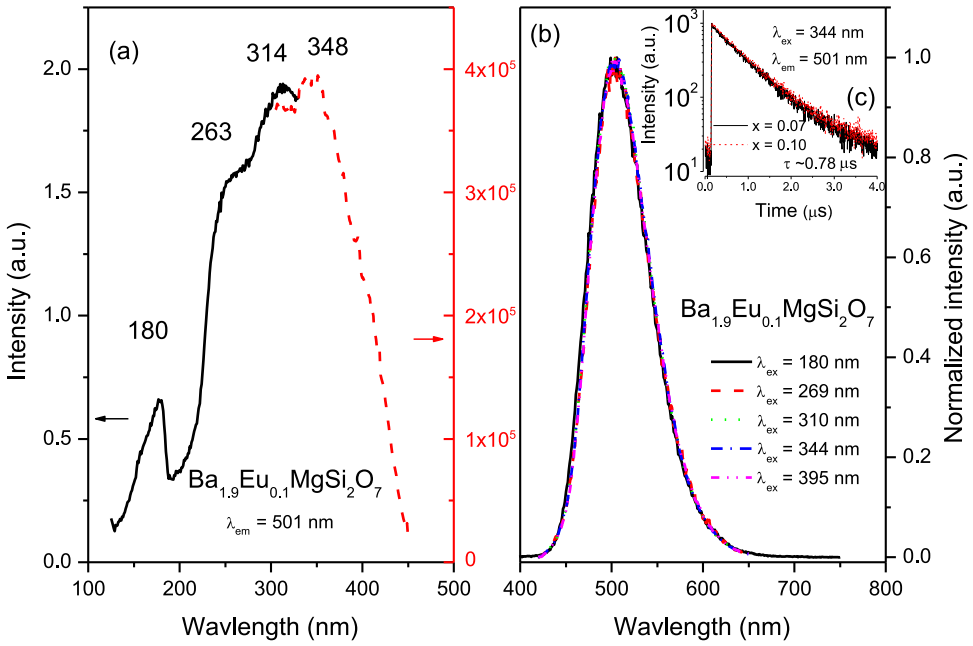

Fig. 3. (a) The synchrotron radiation VUV-UV (black solid line) and lab UV–vis (red dash line) excitation (λ_{em}=501 nm) spectra, (b) the normalized emission (λ_{ex}=180, 269, 310, 344 and 395 nm) spectra of $Ba_{1.9}Eu_{0.1}MgSi_2O_7$ at RT and (c) the decay curves (λ_{ex}=344 nm, λ_{em}=501 nm) of $Ba_{2-x}Eu_xMgSi_2O_7$ (x=0.07, 0.10) at RT. (For interpretation of the references to color in this figure legend, the reader is referred to the web version of this article.)

overlap to the f-d transition bands in principle [23,24]. In addition, the Eu^{3+}-O^{2-} CTB (charge transfer band), whose energy is thought to be close to that of f-d transitions, might occur in this range due to the existence of Eu^{3+} in the sample [25]. Due to all these factors, no separate excitation peaks can be observed. Here, the peaks at 263, 314 and 348 nm are just the comprehensive results of $4f^7 \rightarrow 4f^65d$ transitions of Eu^{2+} and possible CTB in $Ba_2MgSi_2O_7$. Fig. 3(b) displays the normalized emission spectra of $Ba_{1.9}Eu_{0.1}MgSi_2O_7$ under 180, 269, 310, 344 and 395 nm excitation at RT, respectively. Five normalized emission spectra coincide very well with each other, implying that Eu^{2+} ions occupy the same lattice site in the host compound [26]. It is worth to mention that the emission due to f-f transitions of Eu^{3+} is not detected even under 269 (CTB location of Eu^{3+}-O^{2-} in $Ba_{1.98}Eu_{0.01}Na_{0.01}MgSi_2O_7$ at RT, unpublished) and 395 nm ($^7F_0$-$^5L_6$ transitions of Eu^{3+}) excitation in Fig. 3, but the occurrence of Eu^{3+} can be clearly observed in XANES spectrum of Fig. 2. The absorption of Eu L_3 edge in XANES spectrum corresponds to the transition from a $2p_{3/2}$ core level into the continuum state, which relates to atomic weight ratios of ions. The 4f-4f transitions of Eu^{3+} in luminescence spectrum are dependent on the absorption/emission efficiencies. The sample shows green emission due to $4f^65d^1 \rightarrow 4f^7$ transitions of Eu^{2+} and each emission curve is composed of a broad band centered at 504 nm and with a full width at half maximum (FWHM) about 3.07×10^3 cm^{-1}. In addition, the lifetime of Eu^{2+} in $Ba_2MgSi_2O_7$ was measured to be ~0.78 μs at RT as shown in Fig. 3(c).

Fig. 4 shows the temperature dependent emission spectra of $Ba_{1.93}Eu_{0.07}MgSi_2O_7$ under 344 nm excitation in 300–500 K. It can be found that the emission band shifts to the shorter wavelengths and the FWHM increases with increasing temperature. This shift is attributed to lattice expansion at high temperature [11]. It is reasonable to assume that this expanded lattice is an indication of enlargement of the Eu^{2+} site size, accordingly the crystal field strength (CFS) around Eu^{2+} decreases. A weak CFS leads to the increase of the lowest 5d energy of Eu^{2+} ions, therefore gives rise to a shorter wavelengths of the emission band with increasing temperature [27]. Additionally, because the excited electrons spread to high vibration levels at high temperature, the radiative

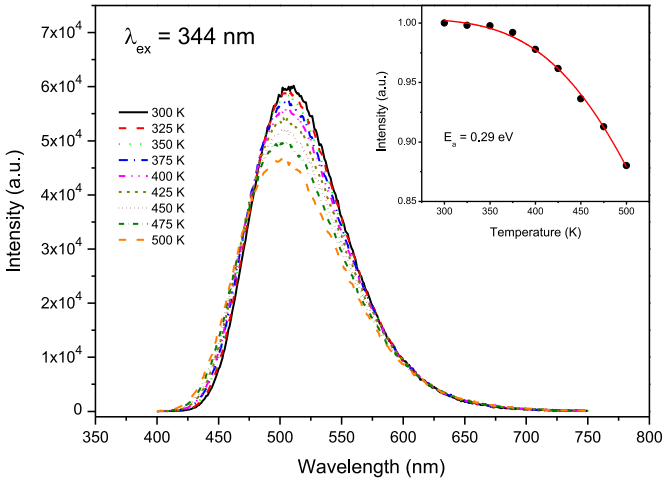

Fig. 4. The emission spectra of $Ba_{1.93}Eu_{0.07}MgSi_2O_7$ under 344 nm excitation at different temperatures from 300 to 500 K. The inset shows the fitted activation energy for thermal quenching.

transitions from these vibration levels result in the increase of FWHMs [11]. The inset of Fig. 4 shows the fitted activation energy for thermal quenching. The quenching data were fitted using the modified Arrhenius Eq. (1) when we assume that the thermal-quenching is due to thermal ionization [28,29],

$$I_T \approx \frac{I_0}{1 + c \ \exp\left(\frac{-E}{kT}\right)} \quad (1)$$

where I_0 is the initial emission intensity, I_T is the intensity at different temperatures, c is a constant for a certain host, k is the Boltzmann constant (8.617×10^{-5} eV), ΔE is activation energy of thermal quenching, corresponding to the energy gap of the lowest 5d excited state of Eu^{2+} in $Ba_2MgSi_2O_7$ and the bottom of the conduction band of $Ba_2MgSi_2O_7$[28,29]. Thus, the activation energy was calculated to be 0.29 eV. This value is significantly smaller than that (~0.64 eV) obtained by fitting the temperature dependent decay time using Arrhenius equation in our pervious

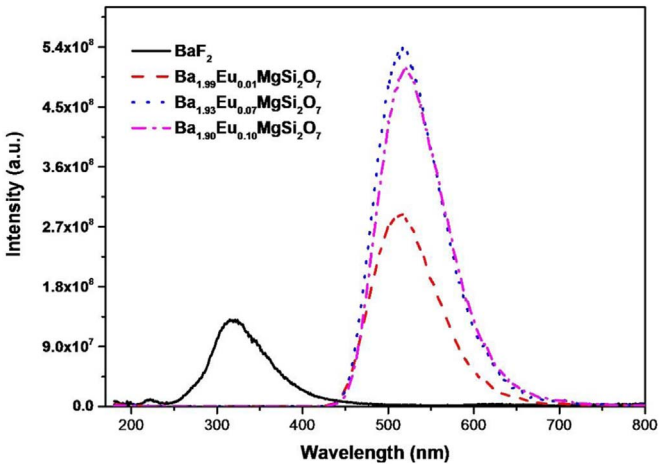

Fig. 5. The X-ray excited emission spectra of $Ba_{2-x}Eu_xMgSi_2O_7$ (x=0.01, 0.07, 0.10) samples and BaF_2 (powder pill) as a reference at RT.

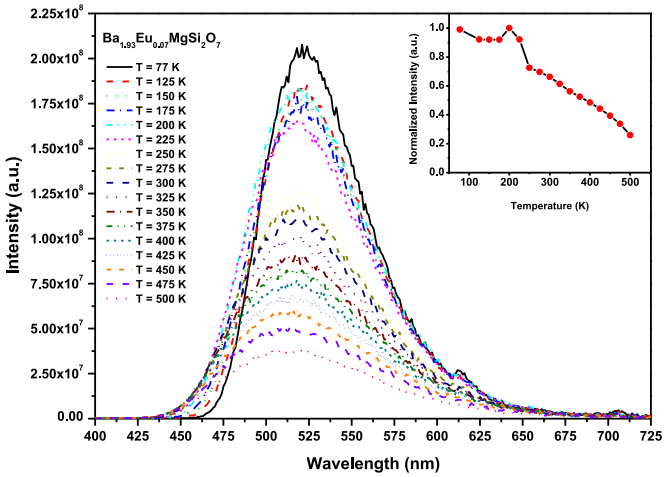

Fig. 6. The X-ray excited emission spectra of the sample $Ba_{1.93}Eu_{0.07}MgSi_2O_7$ at different temperatures, the inset shows temperature dependency of the normalized emission intensity.

paper [7]. Since some factors such as temperature-dependent oscillator strength and distributed scattering centers have considerable influences on the luminescence intensity, we deem that the activation energy obtained by fitting the temperature dependent decay time may be more reliable [29,30].

Fig. 5 gives the X-ray excited emission spectra of $Ba_{2-x}Eu_xMgSi_2O_7$ (x=0.01, 0.07, 0.10) at RT. BaF_2 single crystal and powder sample were measured under the same experimental conditions as a reference sample to obtain an estimate for the absolute emission intensity of our samples [31]. The X-ray excited emission spectra of $Ba_2MgSi_2O_7$:Eu^{2+} display a broad band in the range of 430–700 nm attributed to the $4f^65d^1 \rightarrow 4f^7$ transitions of Eu^{2+}. The shape of the emission band is similar to that under VUV-UV light excitation in Fig. 3(b). The peak of the emission band under X-ray excitation is at a longer wavelength with respect to that under VUV-UV light excitation Fig. 3(b), which is attributed to the different experimental setups. The maximum of emission band shifts from ~510 nm to ~521 nm with increase of Eu^{2+} doping contents from 0.01 to 0.10 due to the enhanced self-absorption at higher doping levels, which is consistent with the photoluminescence behavior [7]. An estimation for the X-ray excited light yield of the samples was determined from the ratio of the integrated intensity (I_{sample}) from those samples (pills) with that of the BaF_2 (I_{BaF2}) reference sample (pill) multiplied with the absolute light yield of BaF_2 single crystal. From the known absolute total light yield of 8880 ph/M eV for BaF_2 reference sample [32–34], the light yield of $Ba_{2-x}Eu_xMgSi_2O_7$ (x=0.01, 0.07, 0.10) samples N_{ph} can be estimated by following Eq. (2):

$$N_{ph} = \frac{\int I_{sample}(\lambda)d\lambda}{\int I_{BaF_2}(\lambda)d\lambda} * 8880\ photons/MeV \quad (2)$$

the X-ray excited light yields of $Ba_{2-x}Eu_xMgSi_2O_7$ (x=0.01, 0.07, 0.10) are estimated to be ~ 16,000 ± 6000, ~ 29,000 ± 6000 and ~ 28,000 ± 6000 ph/M eV, respectively. In consideration of its high scintillation intensity, appropriate decay time and non-hygroscopic property, further optimized $Ba_{1.93}Eu_{0.07}MgSi_2O_7$ may become a promising scintillation material [35–37].

Fig. 6 presents the X-ray excited emission spectra of $Ba_{1.93}Eu_{0.07}MgSi_2O_7$ in temperature range of 77–500 K, which are similar to those measured upon 344 nm excitation in Fig. 4. With increase of temperature, the emission band becomes broader, the emission peak slightly shifts to shorter wavelengths and the emission intensity decreases. In addition, two small peaks appear at ~612 and ~705 nm under low temperatures, which were attributed to the $^5D_0$ – $^7F_2$ and $^5D_0$ – $^7F_4$ transitions of Eu^{3+}, respectively, indicating the existence of Eu^{3+} in this sample and as confirmed by XANES spectrum in Fig. 2. The disappearance of Eu^{3+} emission at high temperature may relate to the different thermal quenching mechanisms of Eu^{2+} and Eu^{3+}, which will be further studied in future. The inset of Fig. 6 shows the normalized integrated intensity of the X-ray excited emission spectra at different temperatures. It is clear that the scintillation intensity decreases with increasing temperature. Near 200 K, the absolute intensity suddenly increases and then quickly decreases again. Such behavior is often associated with the involvement of charge carrier traps in the scintillation process [35,38]. To study further, thermoluminescence spectra were measured.

Fig. 7 displays the thermoluminescence (TL) glow curves of $Ba_{1.93}Eu_{0.07}MgSi_2O_7$. The sample was irradiated for 15 sec with a β-source at a temperature of 90 K. The measurements were done at two different heating rates 1 K/s and 0.5 K/s, respectively. There is a glow peak visible in the 175–280 K range. Depending on the heating rate, the TL curve shows a peak near 216 K or 220 K. At this temperature charge carriers are removed from the traps. Most likely this is the cause of the deviating behaviour near 200 K in Fig. 6. The free charge carriers generated with X-rays at temperature below 200 K are partly trapped and do not participate in the scintillation yield. Near 200 K these charge carriers are liberated and the yield increases. At temperature well above 200 K the traps are not effective anymore and a gradual quenching of scintillation with increase of temperature is observed.

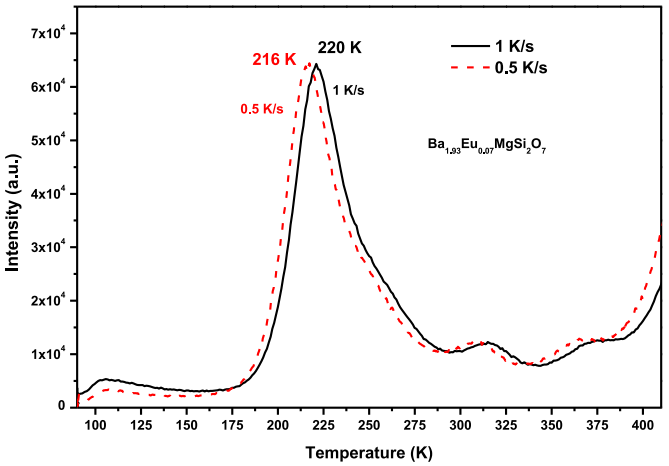

Fig. 7. The thermoluminescence glow curves of $Ba_{1.93}Eu_{0.07}MgSi_2O_7$.

4. Conclusion

In summary, the theoretical density of $Ba_{1.93}Eu_{0.07}MgSi_2O_7$ is calculated to be about 4.36 g/cm^3 according to the refinement result. The XANES spectrum confirms that there are Eu^{2+} and Eu^{3+} in sample $Ba_{1.93}Eu_{0.07}MgSi_2O_7$ prepared in a CO reducing ambient. By a systematic study on luminescence of $Ba_2MgSi_2O_7$:Eu^{2+} under VUV-UV light and X-ray excitation, we have demonstrated that the sample $Ba_{1.93}Eu_{0.07}MgSi_2O_7$ has a high scintillation intensity of $\sim$ 29,000 $\pm$ 6000 ph/M eV upon X-ray excitation. In addition, the effects of temperature on luminescence intensity, band position and FWHM of Eu^{2+} emission of this promising X-ray detecting phosphor are discussed. The results show that the peak of Eu^{2+} emission band slightly shifts to the shorter wavelengths, the FWHM increases accompanied by the decrease of luminescence intensity with increasing temperature. The abrupt increase of light yield at about 200 K relates to the charge carrier traps and this viewpoint is verified by the TL glow curve.

Acknowledgment

This work has been financially supported by the National Natural Science Foundation of China (21171176, U1232108, U1432249, 21671201 and U1632101), and the Natural Science Foundation of Guangdong Province (S2013030012842).

References

[1] C.C. Lin, A. Meijerink, R.-S. Liu, Critical red components for next-generation white LEDs, J. Phys. Chem. Lett. 7 (2016) 495–503.
[2] V.V. Atuchin, N.F. Beisel, E.N. Galashov, E.M. Mandrik, M.S. Molokeev, A. P. Yelisseyev, A.A. Yusuf, Z.G. Xia, Pressure-stimulated synthesis and luminescence properties of microcrystalline $(Lu,Y)_3Al_5O_{12}$:Ce^{3+} garnet phosphors, ACS Appl. Mater. Interfaces 7 (2015) 26235–26243.
[3] P.P. Dai, S.-P. Lee, T.-S. Chan, C.-H. Huang, Y.-W. Chiang, T.-M. Chen, $Sr_3Ce(PO_4)_3$:Eu^{2+}: a broadband yellow-emitting phosphor for near ultraviolet-pumped white light-emitting devices, J. Mater. Chem. C 4 (2016) 1170–1177.
[4] X.G. Zhang, J.L. Zhang, R. Wang, M.L. Gong, Photo-physical behaviors of efficient green phosphor $Ba_2MgSi_2O_7$:Eu^{2+} and its application in light-emitting diodes, J. Am. Ceram. Soc. 93 (2010) 1368–1371.
[5] S.S. Yao, Y.Y. Li, L.H. Xue, Y.W. Yan, Luminescent properties of $Ba_2(Mg,Zn)Si_2O_7$:Eu^{2+} particles as potential blue-green phosphors for ultraviolet light-emitting diodes, J. Am. Ceram. Soc. 93 (2010) 3793–3797.
[6] T.T.H. Tam, N.V. Du, N.D.T. Kien, C.X. Thang, N.D. Cuong, P.T. Huy, N.D. Chien, D. H. Nguyen, Co-precipitation synthesis and optical properties of green-emitting $Ba_2MgSi_2O_7$:Eu^{2+} phosphor, J. Lumin. 147 (2014) 358–362.
[7] J. Yan, L.X. Ning, Y.C. Huang, C.M. Liu, D.J. Hou, B.B. Zhang, Y. Huang, Y. Tao, H. B. Liang, Luminescence and electronic properties of $Ba_2MgSi_2O_7$:Eu^{2+}: a combined experimental and hybrid density functional theory study, J. Mater. Chem. C 2 (2014) 8328–8332.
[8] J. Yan, M.G. Brik, C.M. Liu, D.J. Hou, W.J. Zhou, B.B. Zhang, Y. Huang, Y. Tao, H. B. Liang, VUV-vis photoluminescence, low-voltage cathodoluminescence and electron-vibrational interaction of Mn^{2+} in $Ba_2MgSi_2O_7$, Opt. Mater. 43 (2015) 59–65.
[9] P. Dorenbos, Fundamental limitations in the performance of Ce^{3+}-, Pr^{3+}-, and Eu^{2+}-activated scintillators, IEEE Trans. Nucl. Sci 57 (2010) 1162–1167.
[10] N.J. Cherepy, Strontium and barium iodide high light yield scintillators, Appl. Phys. Lett. 92 (2008) 083508.
[11] C.M. Liu, Z.M. Qi, C.-G. Ma, P. Dorenbos, D.J. Hou, S. Zhang, X.J. Kuang, J. H. Zhang, H.B. Liang, High light yield of $Sr_8(Si_4O_{12})Cl8$:Eu^{2+} under X-ray excitation and its temperature-dependent luminescence characteristics, Chem. Mater. 26 (2014) 3709–3715.
[12] J.P. Zhong, H.B. Liang, Q. Su, J.Y. Zhou, I.V. Khodyuk, P. Dorenbos, Radioluminescence properties of Ce^{3+}-activated $MGd(PO_3)_4$ (M=Li, Na, K, Cs), Opt. Mater. 32 (2009) 378–381.
[13] T. Kim, Y. Kim, S. Kang, Luminescence properties of Eu^{2+} in $M_2MgSi_2O_7$ (M=Ca, Sr, and Ba) phosphors, Appl. Phys. B 106 (2012) 1009–1013.
[14] S. Nishiura, S. Tanabe, Preparation and luminescence properties of glass ceramics precipitated with $M_2MgSi_2O_7$:Eu^{2+} (M=Sr, Ca) phosphor for white light source, IEEE J. Sel. Top. Quantum Electron. 15 (2009) 1177–1180.
[15] I.P. Sahu, D.P. Bisen, N. Brahme, Luminescence properties of green-emitting $Ca_2MgSi_2O_7$:Eu^{2+} phosphor by a solid-state reaction method, Luminescence 30 (2015) 1125–1132.
[16] C.Y. Xu, J.Z. Guo, Y.D. Li, H.J. Seo, Enhanced luminescence of $Ca_2MgSi_2O_7$:Eu^{2+} fibers by sol–gel assisted electrospinning, Opt. Mater. 35 (2013) 893–897.
[17] L. He, B.L. Jia, L.Y. Che, W.S. Li, W.M. Sun, Preparation and optical properties of afterglow $Sr_2MgSi_2O_7$:Eu^{2+}, Dy^{3+} electrospun nanofibers, J. Lumin. 172 (2016) 317–322.
[18] H.Y. Wu, Y.H. Hu, L. Chen, X.J. Wang, Enhancement on the afterglow properties of $Sr_2MgSi_2O_7$: Eu^{2+} by Er^{3+} codoping, Mater. Lett. 65 (2011) 2676–2679.
[19] T. Aitasalo, J. Hölsä, T. Laamanen, M. Lastusaari, L. Lehto, J. Niittykoski, F. Pellé, Crystal structure of the monoclinic $Ba_2MgSi_2O_7$ persistent luminescence material, Z. Krist. 23 (2006) 481–486.
[20] I. Kanno, Y. Yamashita, M. Kimura, F. Inoue, Effective atomic number measurement with energy-resolved X-ray computed tomography, Nucl. Instrum. Methods Phys. Res. Sect. A 787 (2015) 121–124.
[21] Y.H. Wang, D.J. Hou, L. Zhou, H.B. Liang, Y. Huang, Y. Tao, Z. Jiang, Low-voltage cathodoluminescence and Eu/Tb L_3-edge XANES of $Na_{1+y}Ca_{1-x-2y}Eu_xTb_yPO_4$, Opt. Mater. 36 (2014) 839–844.
[22] Y.H. Wang, M.G. Brik, P. Dorenbos, Y. Huang, Y. Tao, H.B. Liang, Enhanced green emission of Eu^{2+} by energy transfer from the $^5D_3$ level of Tb^{3+} in $NaCaPO_4$, J. Phys. Chem. C 118 (2014) 7002–7009.
[23] M. Suta, C. Wickleder, Photoluminescence of $CsMI_3$:Eu^{2+} (M=Mg, Ca, and Sr) – a spectroscopic probe on structural distortions, J. Mater. Chem. C 3 (2015) 5233–5245.
[24] C.K. Duan, M.F. Reid, A simple model for f-d transitions of rare-earth ions in crystals, J. Solid State Chem. 171 (2003) 299–303.
[25] P. Dorenbos, Energy of the Eu^{2+} 5d state relative to the conduction band in compounds, J. Lumin. 128 (2008) 578–582.
[26] C.M. Liu, S. Zhang, Z.Y. Liu, H.B. Liang, S.S. Sun, Y. Tao, A potential cyan-emitting phosphor $Sr_8(Si_4O_{12})Cl_8$:Eu^{2+} for wide color gamut 3D-PDP and 3D-FED, J. Mater. Chem. C 1 (2013) 1305–1308.
[27] Y. Sato, H. Kato, M. Kobayashi, T. Masaki, D.-H. Yoon, M. Kakihana, Tailoring of deep-red luminescence in Ca_2SiO_4:Eu^{2+}, Angew. Chem. Int. Ed. 53 (2014) 7756–7759.
[28] P. Dorenbos, Thermal quenching of Eu^{2+} 5d–4f luminescence in inorganic compounds, J. Phys. : Condens. Matter 17 (2005) 8103–8111.
[29] R. Shi, J.Z. Xu, G.K. Liu, X.J. Zhang, W.J. Zhou, F.J. Pan, Y. Huang, Y. Tao, H. B. Liang, Spectroscopy and luminescence dynamics of Ce^{3+} and Sm^{3+} in $LiYSiO_4$, J. Phys. Chem. C 120 (2016) 4529–4537.
[30] V. Bachmann, C. Ronda, O. Oeckler, W. Schnick, A. Meijerink, Color point tuning for (Sr, Ca, Ba)$Si_2O_2N_2$: Eu^{2+} for white light LEDs, Chem. Mater. 21 (2009) 316–325.
[31] W.J. Zhou, D.J. Hou, F.J. Pan, B.B. Zhang, P. Dorenbos, Y. Huang, Y. Tao, H. B. Liang, VUV-vis photoluminescence, X-ray radioluminescence and energy transfer dynamics of Ce^{3+} and Pr^{3+} doped $LiCaBO_3$, J. Mater. Chem. C 3 (2015) 9161–9169.
[32] X.M. Ding, H.B. Liang, D.J. Hou, Q. Su, P. Dorenbos, S.S. Sun, Y. Tao, Ultraviolet-vacuum ultraviolet photoluminescence and X-ray radioluminescence of Ce^{3+}-doped $Ba_3MgSi_2O_8$, J. Appl. Phys. 110 (2001) 113522.
[33] D.J. Hou, W.J. Zhou, C. Wu, P. Dorenbos, H.B. Liang, T.-K. Sham, B.B. Zhang, Y. Huang, Y. Tao, Luminescence and X-ray absorption studies on 0.5% Ce^{3+} doped $BaCa_2MgSi_2O_8$ phosphor, Phys. Chem. Chem. Phys. 17 (2015) 22035–22041.
[34] D.J. Hou, B. Han, W.P. Chen, H.B. Liang, Q. Su, P. Dorenbos, Y. Huang, Z.H. Gao, Y. Tao, Luminescence of Ce^{3+} at two different sites in α-$Sr_2P_2O_7$ under vacuum ultraviolet-UV and X-ray excitation, J. Appl. Phys. 108 (2010) 083527.
[35] M.S. Alekhin, D.A. Biner, K.W. Krämer, P. Dorenbos, Optical and scintillation properties of $CsBa_2I_5$:Eu^{2+}, J. Lumin. 145 (2014) 723–728.
[36] Y.T. Wu, L.A. Boatner, A.C. Lindsey, M. Zhuravleva, S. Jones, J.D. Auxier II, H. L. Hall, C.L. Melcher, Defect engineering in SrI_2:Eu^{2+} single crystal scintilla, Cryst. Growth Des. 15 (2015) 3929–3938.
[37] S.P. Liu, X.Q. Feng, J.A. Mares, V. Babin, M. Nikl, A. Beitlerova, Y. Shi, Y.P. Zeng, Y. B. Pan, C. D'Ambrosio, Y.H. Huang, Optical, luminescence and scintillation characteristics of non-stoichiometric LuAG:Ce ceramics, J. Lumin. 169 (2016) 72–77.
[38] G. Patton, F. Moretti, A. Belsky, K.A. Saghir, S. Chenu, G. Matzen, M. Allix, C. Dujardin, Light yield sensitization by X-ray irradiation of the $BaAl_4O_7$:Eu^{2+} ceramic scintillator obtained by full crystallization of glass, Phys. Chem. Chem. Phys. 16 (2014) 24824–24829.